IOP Publishing Plasma Physics and Controlled Fusion

Plasma Phys. Control. Fusion **56** (2014) 075001 (6pp) doi:10.1088/0741-3335/56/7/075001

Numerical experiments on neutron yield and soft x-ray study of a ∼100 kJ plasma focus using the current profile fitting technique

S T Ong[1], K Chaudhary[1], J Ali[1,*] and S Lee[2,3]

[1] Institute of Advanced Photonics Science, Nanotechnology Research Alliance, Universiti Teknologi Malaysia, UTM Johor Bahru, 81310 Johor, Malaysia
[2] Centre for Plasma Research, INTI International University, 71800 Nilai, Malaysia
[3] Institute for Plasma Focus Studies, 32 Oakpark Drive, Chadstone 3148, Australia

E-mail: djxxx_1@yahoo.com

Received 13 December 2013, revised 23 February 2014
Accepted for publication 27 March 2014
Published 8 May 2014

Abstract

Numerical experiments using the Lee model were performed to study the neutron yield and soft x-ray emission from the IR-MPF-100 plasma focus using the current fitting technique. The mass sweeping factor and the current factor for the axial and radial phase were used to represent the imperfections encountered in experiments. All gross properties including the yields were realistically simulated once the computed and measured current profiles were well fitted. The computed neutron yield Y_n was in agreement with the experimentally measured Y_n at 20 kV ($E_0 \sim 30$ kJ) charging voltage. The optimum computed neutron yield of $Y_n = 1.238 \times 10^9$ neutrons per shot was obtained at optimum physics parameters of the plasma focus operated with deuterium gas. It was also observed that no soft x-rays were emitted from the IR-MPF-100 plasma focus operated with argon gas due to the absence of helium-like and hydrogen-like ions at a low plasma temperature (∼0.094 keV) and axial speed (8.12 cm μs^{-1}). However, the soft x-ray yield can be achieved by increasing the charging voltage, using a higher ratio of outer anode radius to inner anode radius c or shorter anode length z_0, or using neon as the operating gas.

Keywords: numerical experiments, Lee model, plasma focus, neutron yield, soft x-ray, deuterium, argon

(Some figures may appear in colour only in the online journal)

1. Introduction

Mather-type plasma focus devices comprising of a set of cylindrical electrodes have been extensively used as a source of multi-radiation such as neutron yield [1], soft [2] and hard [3] x-rays, high energy electrons [4] and ion beams [5]. A high-voltage pulsed discharge between the electrodes through the selected gas medium produces a current sheath at the base of the cathode, which is then axially driven by a Lorentz force and leads to the strong electromagnetic compression of the plasma at the flat top of the anode [6]. A column of plasma pinch is formed and then finally disrupted, resulting in the emission of high-energy particles and intense radiations.

Due to its potential in many applications, scientists have pursued the optimum conditions for radiation yields and the usability of the plasma focus device. Neutron yield [1, 7–9] and soft x-ray [2, 10] investigations of the plasma focus are among the popular research topics that has been numerically and experimentally studied in many aspects. Verma *et al* [1]. reported the neutron yield characteristics and optimization for

* Author to whom any correspondence should be addressed.

the ~20 kJ NX-3 plasma focus device operated with deuterium gas using the ordinary anode of radius $a = 20$ mm and length $z = 160$ mm. The average yield in the order of $\sim 10^9$ neutrons per shot was obtained. The highest yield of $\sim 4.6 \times 10^9$ neutrons per shot was achieved at 6 mbar with 14 kV discharge voltage. The device was further optimized by varying the anode configuration. The average peak neutron yield was increased from $(2.38 \pm 0.31) \times 10^9$ neutrons per shot to $(3.40 \pm 0.43) \times 10^9$ neutrons per shot for the anode with radius and length of 26 mm and 140 mm, respectively. Kies [11] and Herold [12] individually presented the scaling law of neutron yield ($Y_n \sim I_{pinch}^{3.2}$ to $\sim I_{pinch}^4$) by compiling the experimental data from the plasma focus machines over a wide range of energies. However, there was uncertainty with this scaling law because the recorded I_{pinch} from those experimental data were inaccurately measured, or estimated from the total peak current. Lee *et al* [7]. presented the numerical neutron scaling laws using the Lee computational model, in which the I_{pinch} was rigidly computed. A calibration point was derived from the laboratory data before carrying out the numerical experiment. The current fitting technique was used to obtain the properties of selected plasma focus machines. The numerically derived neutron scaling laws were found to be $Y_n \sim I_{pinch}^{4.7}$ and $Y_n \sim I_{peak}^{3.9}$ (both in the order of MA). The study suggested that the scaling of Y_n versus I_{pinch} is more reliable and robust compared to the scaling of Y_n versus I_{peak}, as there is a value for I_{peak} even at non-optimized conditions (even when Y_n is zero). In addition, the Lee model has also been used in other studies to obtain the neutron yield versus pressure and compared with experimental data [8], and in a numerical study of the neutron yield saturation effect [9].

In addition to the investigations into various aspects of neutron yield, soft x-ray emission from plasma focus has also been continually studied by researchers. Soft x-ray emission has been observed and investigated by Bayley *et al* [2]. using the 70 kJ SPEED 2 plasma focus machine. Argon gas was injected into the deuterium-filled plasma focus chamber from the anode tip before the discharge to ensure the formation of plasma pinch and hence the emission of argon soft x-rays. The gas pressure of the deuterium was about 4 hPa (~3 Torr) and the plenum pressure of the argon gas was 0.35 MPa. Time-resolved and time-integrated diagnostic instruments were used for the space and spectral investigations of soft x-ray yield. The total soft x-ray yield (at a wavelength range between 0.2 and 1.2 nm) was recorded at several tens of Joules per shot. Most of the soft x-rays were emitted from short-lived (~0.25 ns) pinch-like hotspots. Gates [13] suggested the scaling rule of x-rays yield to be $Y_x \sim I_{peak}^4/(r_p)^2$, where r_p is the pinch radius. The I_{peak} may be calculated for a given capacitor bank, but the quantification of the pinch radius is difficult as the radius keeps changing during the pinching [6]. Akel and Lee [10]. have reported the scaling of optimized argon soft x-ray yield of plasma focus. The Lee model code was used to conduct a series of numerical experiments for storage energies, E_0, ranging from 1 kJ to 1 MJ and operated at 1 Torr argon gas pressure. The scaling was found to be $Y_{SXR} \sim I_{pinch}^{4.1}$ for high-inductance plasma focus (270 nH) and $Y_{SXR} \sim I_{pinch}^{4.9}$ for low-inductance plasma focus (10 nH).

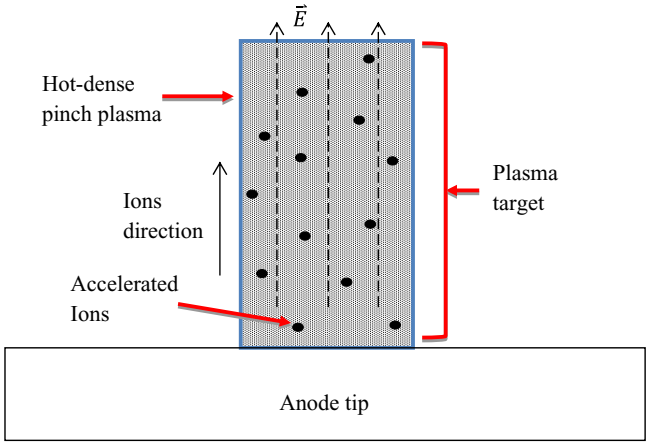

Figure 1. Schematic diagram of beam-target neutron yield mechanism.

Recently, the preliminary results of a newly built 115 kJ IR-MPF-100 plasma focus device were presented by Salehizadeh *et al* [14]. The device consisted of a brass anode 22 cm in length with a radius of 6.25 cm. Twelve copper cathodes the same length as the anode surrounded the anode with a radius of 10.2 cm. The device was operated by a total of 24 6 μF capacitors connected in parallel with each other that can be charged up to 40 kV. The static inductance of the device was estimated at around 120 nH. The voltage, current, and current derivative signals were measured and recorded. The device was operated in a deuterium and argon ambient environment. For the operation at 20 kV ($E_0 \sim 30$ kJ) and 1.9 Torr deuterium pressure, a total of $\sim 1.5 \times 10^9$ neutrons per shot was measured using a neutron activation counter. However, the pressure was not yet in an optimized state for neutron emission and, for the operation in argon, there is in fact significant soft x-ray emission from plasma focus reported in previous experiments [2, 10].

In this paper, the Lee model code [15] is used as a basis for the current fitting technique, in order to simulate the conditions of the IR-MPF-100 plasma focus realistically. In the meantime, the computed neutron yield Y_n is optimized as a function of pressure. The total soft x-ray emission in the operation of argon filling gas from the published current profile is also investigated [14]. Lee's model couples up the dynamics of the plasma current sheath and pinch, thermodynamics and radiation with electric circuit equations, which enables the realistic simulation of the plasma focus electrodynamic properties. It has been extensively applied to different plasma focus devices within a wide range of energies [16]. The beam–target mechanism of the neutron yield was described by Gribkov *et al* [17]. The 'beam' refers to the non-thermal highly energetic ion beam, which is accelerated by the strong electric fields caused by the instabilities during the pinching [18]. The 'target' refers to the hot dense plasma in the pinch column, which is formed by the self-generated imploding $J \times B$ force. Figure 1 shows the schematic diagram of the neutron yield mechanism.

The interaction between the beam and target leads to the emission of neutrons and other fusion products. The

beam–target neutron yield can be determined as [7, 8, 15]:

$$Y_{b-t} = C_n n_i I_{pinch}^2 z_p^2 \left(\ln\left(b/r_p\right)\right) \sigma / U^{0.5}, \quad (1)$$

where n_i is the ion number density, I_{pinch} is the initial pinch current, z_p is the pinch length, r_p is the pinch radius, b is the radius of the circle formed by the cathodes, σ is the cross-section of deuterium–deuterium (D–D) fusion reaction (neutron branch) [19], and C_n is the calibration constant obtained by calibrating the yield [7, 8, 15] from the compiled laboratory data. The computed U (in keV) is equal to three times the induced voltage, V_{max} (the induced voltage in kV drives the deuteron of charge e to an energy of V_{max} keV), which is around 45–150 keV. The D–D cross-section is reasonably obtained with V_{max} multiplied by 3, based on the experimental data reported by Lee *et al* [8].

The soft x-ray emission is calculated by subtracting the plasma self-absorption from the generated soft x-ray energy (line radiation), which mainly depends on the temperature and density. This effect is caused by the reabsorption of an emitted photon (in this case, the soft x-ray) from an atom/ion by another plasma component before escaping the plasma region, resulting in a lower radiation yield. The rate of argon line radiation can be calculated as follows [15]:

$$\frac{dQ_L}{dt} = -4.6 \times 10^{-31} n_i^2 Z_{eff} Z_n^4 \left(\pi r_p^2\right) z_p / T, \quad (2)$$

where n_i is the ion number density, Z_{eff} is the effective charge number, Z_n is the atomic number, r_p and z_p are the pinch radius and pinch length, respectively, and T is the plasma pinch temperature. Q_L can be obtained by integration over the pinching period. The balance quantity after the reduction of self-absorption is emitted as a soft x-ray. This effect is included in the model calculation [15] even though it is insignificant for operation in low-pressure argon [20], i.e. $Y_{SXR} = Q_L$. It is important to note that for operation in different gases, there is a specific range of plasma temperatures (temperature window) required for the emission of soft x-rays. The experimental studies reported by Shan [21] proved that the x-rays from argon plasma are mainly emitted by Ar^{16+} (helium-like) and Ar^{17+} (hydrogen-like) ions. The specific range of electron temperatures for the ionizations of Ar^{16+} and Ar^{17+} ions is between 1.4 and 5 keV (1.625×10^7 to 5.802×10^7 K). From the numerical experiment of x-ray scaling [10], the range of axial speed for argon soft x-ray yield in plasma focus is around 11–14 cm μs^{-1}.

2. Current fitting technique using the Lee model code

In general, the Lee code [15] simulates the development process of the current sheath in three main phases: the breakdown, the axial and the radial phase [6]. According to Lee [7], when the computed current profile is reasonably fitted to the measured current profile, then all gross physical properties in the plasma focus can be simulated in a realistic manner. This can be done by inputting the bank parameters (such as inductance, L_0; capacitance, C_0; stray resistance, r_0), the tube parameters (radius of the cathode,b; anode radius, a; anode length,z_0) and operational parameters (charging voltage, V_0; gas pressure, P_0; and filling gas). The actual situation in experiments is not as ideal as in the simulation, causing the computed current trace and measured current trace not to be fitted at any gradient. Therefore, the four model parameters f_m, f_c, f_{mr} and f_{cr} are included into the electrodynamics of the system, where f_m and f_c are the mass sweeping factor and the current factor for the axial phase; f_{mr} and f_{cr} likewise for the radial phase. f_m accounts for all the phenomena that caused the mass sweeping defects. f_c accounts for the fraction of current flow into the plasma sheath. Likewise for f_{mr} and f_{cr}, where the former is used to account for the variations of the amount of mass in the plasma column and the latter accounts for the fraction of current flow in the imploding structure.

Table 1. The bank, tube and operational parameters of IR-MPF-100 [14].

Bank parameters			Tube parameters			Operational parameters		
							P_0 (Torr)	
L_0 (nH)	C_0 (μF)	r_0 (mΩ)	b (cm)	a (cm)	z_0 (cm)	V_0 (kV)	D_2	Ar
120 (estimated)	144	5	10.2	6.25	22	20	1.9	0.3

These model parameters are then adjusted one by one to fit the computed current profile to the measured one, with fixed tube, operational and bank parameters. Due to the fact that in many experiments the bank parameters are given with their estimation, most of the time the adjustments of bank parameters are also required to achieve current matching. Once the computed current profile is fitted with the measured current profile, the model is set up for the real conditions of the specific plasma focus device and the model parameters are fixed to conduct the other numerical experiments.

3. Numerical experiment and discussion

In a recent paper [14], the current signals for ambient pressure 1.9 Torr deuterium and 0.3 Torr argon for the IR-MPF-100 plasma focus have been presented. Both of the published current signals were measured at 20 kV discharge voltages and operated under the same conditions, with the exception of the ambient gas and pressure. The current fitting technique is then applied to the different measured current profiles separately. The code is configured using the published parameters shown in table 1.

First, the computed current profile is fitted to the measured deuterium (D_2) current profile. The model is prepared to perform the fitting with the published parameters. The values of model parameters f_m, f_c, f_{mr} and f_{cr} are ignored in the first step. Then the f_m and f_c factors for the axial phase are adjusted until the slope and the peak of the computed current trace are reasonably fitted to the measured current trace. The adjustment of the f_{mr} and f_{cr} factors is performed for the radial phase until the slope and depth of the computed current dip fit with the measured current dip. However, according to previous cases of fitting in other papers [7, 8], due to the sensitivity of the fitting process, if any of the bank parameters are given incorrectly, the

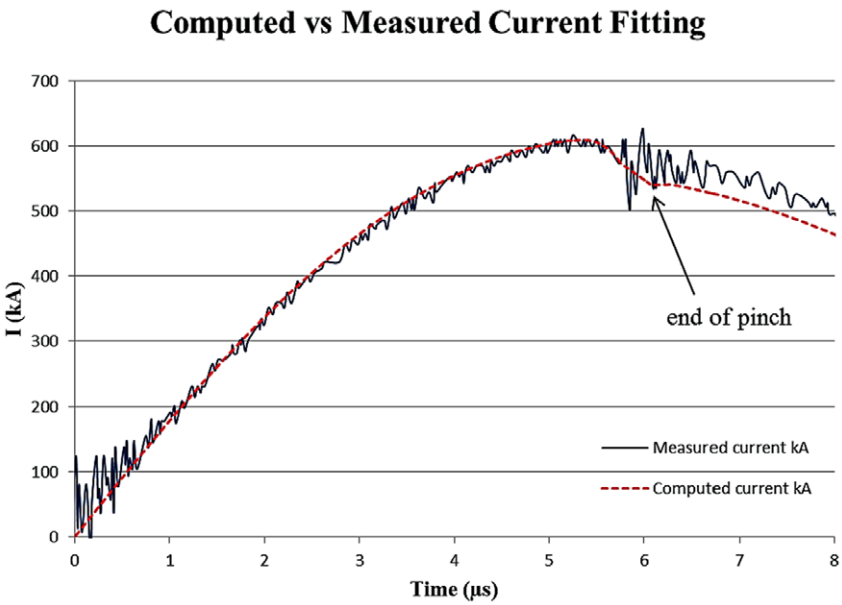

Figure 2. Comparison of computed and measured current profile for 1.9 Torr deuterium gas.

Table 2. Computed properties of the IR-MPF-100 plasma focus, where P_0 = gas pressure (deuterium), Y_n = neutron yield, I_{peak} = peak total current, I_{pinch} = initial pinch current, T_{pinch} = pinch temperature, v_a = axial speed, v_s = radial shock speed, v_p = radial piston speed, r_{min} = minimum pinch radius, z_{max} = maximum pinch column length, 'Pinch dur' = pinch duration, V_{max} = maximum induced voltage, and n_i = ion number density. The first and second rows of bold values represent the set of values obtained from the current fitting and the set of values with optimum neutron yields, respectively.

P_0 (Torr)	Y_n (10^9 neutrons)	I_{peak} (kA)	I_{pinch} (kA)	Min T_{pinch} (10^6)	Max T_{pinch} (10^6)	Peak v_a (cm/μs)	Peak v_s (cm/μs)	Peak v_p (cm/μs)	r_{min} (cm)	z_{max} (cm)	Pinch dur (ns)	V_{max} (kV)	n_i (10^{23}/m^3)
0.7	0.582	541	232	3.99	4.12	10.1	17.7	11.7	0.67	7.2	79.4	33.3	1.6
1.0	0.814	569	243	3.05	3.15	8.9	15.4	10.2	0.67	7.2	91.2	30.2	2.3
1.2	0.941	582	247	2.63	2.72	8.4	14.4	9.4	0.67	7.2	98.1	28.7	2.7
1.5	1.093	597	251	2.16	2.25	7.8	13.2	8.6	0.68	7.1	107.3	26.7	3.3
1.7	1.160	603	253	1.93	2.01	7.4	12.5	8.1	0.68	7.1	113.9	25.3	3.7
1.9	**1.208**	**609**	**254**	**1.73**	**1.81**	**7.1**	**11.9**	**7.7**	**0.69**	**7.1**	**119.8**	**24.1**	**4.1**
2.0	1.222	611	254	1.65	1.73	7.0	11.6	7.5	0.69	7.1	123.1	23.5	4.3
2.1	1.233	613	254	1.57	1.64	6.9	11.4	7.3	0.69	7.1	126.1	22.9	4.5
2.2	**1.238**	**615**	**254**	**1.49**	**1.57**	**6.7**	**11.1**	**7.2**	**0.69**	**7.1**	**129.0**	**22.4**	**4.7**
2.3	1.237	617	254	1.43	1.50	6.6	10.9	7.0	0.69	7.1	132.3	21.8	4.9
2.4	1.231	618	254	1.36	1.43	6.5	10.6	6.8	0.70	7.1	135.5	21.3	5.1
2.6	1.211	621	253	1.24	1.31	6.3	10.2	6.6	0.70	7.1	141.2	20.4	5.4
2.8	1.176	623	252	1.14	1.21	6.1	9.9	6.3	0.70	7.1	147.5	19.4	5.8
3.2	1.069	626	248	0.96	1.03	5.8	9.2	5.8	0.71	7.1	159.6	17.7	6.4
3.6	0.926	628	244	0.82	0.88	5.5	8.5	5.4	0.73	7.1	173.0	16.1	7.0
4.2	0.687	631	236	0.65	0.71	5.1	7.7	4.9	0.75	7.0	193.7	13.9	7.7

computed current trace cannot be fitted to the measured current trace for any adjusted values of the four model parameters.

In this article, the model parameters are: $f_m = 0.089$, $f_c = 0.49$, $f_{mr} = 0.42$ and $f_{cr} = 0.46$. L_0 and r_0 are varied to achieve a typical agreement between the computed and measured current profiles. The following parameters are fixed for computation: bank parameters: $L_0 = 109$ nH, $C_0 = 144\,\mu$F, $r_0 = 3\,$mΩ; tube parameters: $b = 10.2$ cm, $a = 6.25$ cm, $z_0 = 22$ cm; operational parameters: $V_0 = 20$ kV, $P_0 = 1.6$ Torr (deuterium). To resolve the time delay of the spark gap switching in the experiment as compared to the instantaneous switching of the code, a time shift is made to the computed current profile. The fitted graph for computed and measured current profiles is shown in figure 2.

From figure 2, it is observed that the computed current profile (dotted line) is very well fitted to the measured current profile (solid noisy line) from the start of the current breakdown to the end of the pinch (as indicated in figure 2). Once it is fitted, then all gross physical properties in the plasma focus, including the yields, are realistically simulated. To obtain the optimized neutron yield, Y_n, the configured model is then used to conduct the numerical experiments at various deuterium pressures at a charging voltage of 20 kV. The pressure is varied until a maximum Y_n is obtained. The neutron yield Y_n and other computed properties are tabulated in table 2. A graph of the neutron yield as a function of pressure is shown in figure 3.

In table 2, the computed Y_n for 1.9 Torr deuterium gas is 1.208×10^9 neutrons per shot; this is in good agreement with

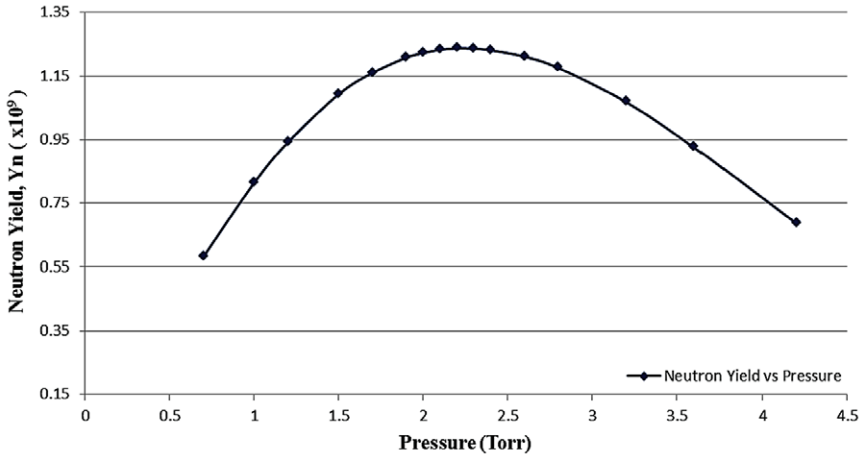

Figure 3. The computed neutron yield, Y_n, versus pressure, P_0.

the experimentally measured Y_n of the IR-MPF-100 plasma focus, which is around 1.50×10^9 neutrons per shot. The optimum computed neutron yield is increased by 3×10^7 neutrons per shot to 1.238×10^9 neutrons per shot at the pressure of 2.2 Torr, with a similar initial pinch current, I_{pinch}, to the computed Y_n at 1.9 Torr.

Note that the optimized Y_n at 2.2 Torr has a smaller range of pinch temperatures and slower peak v_a, v_s and v_p compared to the 1.9 Torr computed shot. The lower pinch temperature obtained with the 2.2 Torr shot is due to the slower current sheath speed as the temperature is directly proportional to the square of the radial pinch speed (v_s and v_p) and correlated to the value of the axial speed, v_a. The axial speed of the current sheath is inversely proportional to the square root of pressure, P_0, causing the current sheath speed to decrease at higher P_0 [15], indicating that the speed of the current sheath is not the dominant factor contributing to the neutron yield, Y_n [18]. In fact, the increase in pressure in a static volume (i.e., the increase in gas density) leads to an increase in ion density, n_i, which has a linear relationship to Y_n. However, Y_n decreases with the further increase in P_0 (as shown in figure 3), as the increase in P_0 delays the plasma focus pinch, leading to the lower initial pinch current, I_{pinch} ($Y_n \sim I_{pinch}^2$). Therefore, an optimized Y_n can only be obtained once the optimum physical properties of the plasma focus are achieved. A similar approach might be used in the experiment of the IR-MPF-100 plasma focus so that more comparisons can be made for detailed studies.

The numerical experiment on soft x-ray emission is then conducted on the IR-MPF-100 plasma focus operated at 0.3 Torr argon pressure. The computed current profile is calculated to fit with the measured one using the configured bank parameters as in the previous case of deuterium current profile fitting. The following parameters are fixed for computation: bank parameters: $L_0 = 109$ nH, $C_0 = 144\,\mu$F, $r_0 = 3\,$mΩ; tube parameters: $b = 10.2$ cm, $a = 6.25$ cm, $z_0 = 22$ cm; operational parameters: $V_0 = 20$ kV, $P_0 = 0.3$ Torr (Ar); with consideration of the model parameters as follows: $f_m = 0.031$, $f_c = 0.43$, $f_{mr} = 0.165$ and $f_{cr} = 0.11$. The fitted computed and measured current profiles are shown in figure 4.

From figure 4, it can be observed that the computed current profile (dotted line) is fitted very well (on average) to the measured current profile (solid noisy line) until the end of the pinch. The well-fitted current profile indicates that all gross physical properties in the IR-MPF-100 plasma focus are realistically simulated in the model, including the neutrons and x-ray yields. Thus, the argon soft x-ray emission can be determined from the model. However, the maximum plasma temperature is recorded as 1.09×10^6 K (~0.094 keV) at an axial speed of 8.12 cm μs^{-1}. The dominant ions are mainly Ar^{10+}, Ar^{11+}, Ar^{12+} and Ar^{13+} for this particular temperature, as reported in the Corona model [21]. In this case, no soft x-rays are emitted from the IR-MPF-100 plasma focus as the emission requires the presence of helium-like and hydrogen-like ions. Unlike the neutron yield, soft x-ray emission is strongly correlated to the pinch temperature and the current sheath speed. A higher axial speed is required to heat up the pinched plasma to the temperature window of about 1.6×10^7 to 5.8×10^7 K (1.4 to 5 keV). This can be achieved by:

(a) Increasing the operating charging voltage so that more energy will be injected into the system;
(b) Using a higher ratio of c ($c = b/a$) or a shorter z_0 compared to the c of the IR-MPF-100 plasma focus ($c = 1.6$, $z_0 = 22$ cm) by reducing the anode radius;
(c) Using different operating gases. It is shown that neon gas is a better source of soft x-ray yield as it requires lower electron temperatures (200–500 eV) for the ionization state of Ne^{8+} and Ne^{9+} (helium-like and hydrogen-like ions) [22].

4. Conclusion

Numerical experiments with the current fitting technique were applied to the measured current profile of 1.9 Torr deuterium and 0.3 Torr argon for the IR-MPF-100 plasma focus. Both of the computed current profiles for the respective shots were well fitted to the measured ones, allowing realistic simulations of the gross properties in the plasma focus. For the operation in deuterium gas, the optimum computed neutron yield is 1.238×10^9 neutrons per shot at a gas pressure of 2.2 Torr.

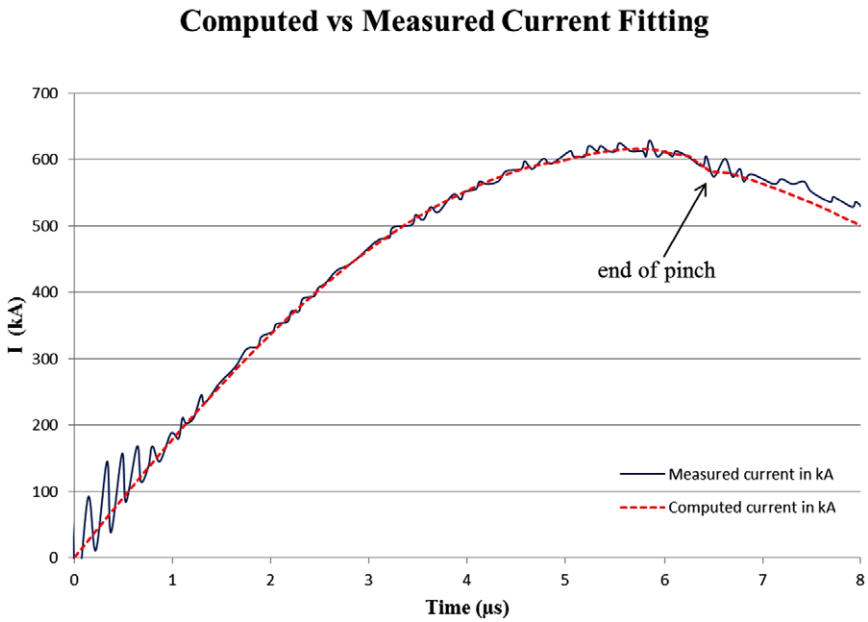

Figure 4. Comparison of computed and measured current profile for 0.3 Torr argon gas.

It was found that the further increase in pressure leads to a lower I_{pinch} and hence a lower yield as $Y_{\text{n}} \sim I^2_{\text{pinch}}$. The maximum Y_{n} was achieved at optimum operational physical properties of the plasma focus. In the case of argon gas, no soft x-rays were emitted from the IR-MPF-100 plasma focus due to the lower plasma temperature (∼0.094 keV) and axial speed (8.12 cm μs^{-1}), which were insufficient to ionize the argon gas to helium-like and hydrogen-like ions. However, the desired plasma temperature and axial speed can be achieved by increasing the charging voltage, using a higher ratio of outer anode radius to inner anode radius c or a shorter anode length z_0, or using neon as the operating gas.

References

[1] Verma R *et al* 2012 Neutron emission characteristics of NX-3 plasma focus device: speed factor as the guiding rule for yield optimization *IEEE Trans. Plasma Sci.* **40** 3280–9

[2] Bayley J M *et al* 1991 Observations of soft-x-ray production in the speed-2 plasma-focus *J. Appl. Phys.* **69** 613–7

[3] Castillo-Mejia F *et al* 2001 Small plasma focus studied as a source of hard x-ray *IEEE Trans. Plasma Sci.* **29** 921–6

[4] Patran A *et al* 2005 Spectral study of the electron beam emitted from a 3 kJ plasma focus *Plasma Sources Sci. Technol.* **14** 549–60

[5] Lee S and Saw S H 2013 Plasma focus ion beam fluence and flux—for various gases *Phys. Plasmas* **20** 062702

[6] Saw S H *et al* 2012 Magnetic probe measurements in INTI plasma focus to determine dependence of axial speed with pressure in neon *J. Fusion Energy* **31** 411–7

[7] Lee S and Saw S H 2008 Neutron scaling laws from numerical experiments *J. Fusion Energy* **27** 292–5

[8] Lee S *et al* 2009 Numerical experiments on plasma focus neutron yield versus pressure compared with laboratory experiments *Plasma Phys. Control. Fusion* **51** 075006

[9] Lee S 2009 Neutron yield saturation in plasma focus: a fundamental cause *Appl. Phys. Lett.* **95** 151503

[10] Akel M and Lee S 2012 Dependence of plasma focus argon soft x-ray yield on storage energy, total and pinch currents *J. Fusion Energy* **31** 143–50

[11] Kies W 1986 Plasma focus—physics and technology *Proc. 2nd Tropical College on Applied Physics: Laser and Plasma Technology (University of Malaya, Malaysia, 1988)* (Singapore: World Scientific) pp 86–137

[12] Herold H 1988 Physics and technology of large plasma focus devices *Proc. 3rd Tropical College on Applied Physics: Laser and Plasma Technology (University of Malaya, Malaysia, 1990)* (Singapore: World Scientific) pp 21–45

[13] Gates D C 1978 *Proc. 2nd Int. Conf. on Energy Storage, Compression and Switching (Venice, Italy, 1983)* (New York: Plenum) pp 329–51

[14] Salehizadeh A *et al* 2013 Preliminary results of the 115 kJ dense plasma focus device IR-MPF-100 *J. Fusion Energy* **32** 293–7

[15] Lee S 2013 Radiative dense plasma focus computation package: RADPF [October 2013] www.plasmafocus.net/IPFS/modelpackage/File1RADPF.htm

[16] Lee S *et al* 2011 Characterizing plasma focus devices—role of the static inductance—instability phase fitted by anomalous resistances *J. Fusion Energy* **30** 277–82

[17] Gribkov V A *et al* 2007 Plasma dynamics in the PF-1000 device under full-scale energy storage: II. Fast electron and ion characteristics versus neutron emission parameters and gun optimization perspectives *J. Phys. D: Appl. Phys.* **40** 3592–607

[18] Koh J M *et al* 2005 Optimization of the high pressure operation regime for enhanced neutron yield in a plasma focus device *Plasma Sources Sci. Technol.* **14** 12–8

[19] Huba J D 2011 NRL Plasma Formulary [November 2013] www.ppd.nrl./navy.milnrlformulary/NRL_FORMULARY_07.pdf

[20] Wong D *et al* 2004 Soft x-ray optimization studies on a dense plasma focus device operated in neon and argon in repetitive mode *IEEE Trans. Plasma Sci.* **32** 2227–35

[21] Shan B 2000 Plasma dynamics and x-ray emission of the plasma focus *NIE* (Singapore: Nanyang Technological University) ICTP Open Access Archive http://eprints.ictp.it/99/

[22] Liu M 2006 Soft x-rays from compact plasma focus *NIE* (Singapore: Nanyang Technological University) ICTP Open Access Archive http://eprints.ictp.it/327/